

High Resolution Low Energy Electron Diffraction Study of Flattening on the TiO₂(110) Surface

Bruno Grossmann and Peter Piercy

Department of Physics, University of Ottawa, Ottawa, Ontario, Canada K1N 6N5

(Received 21 December 1994)

We investigate the thermal annealing of a TiO₂ surface on atomic length scales using high resolution low energy electron diffraction (spot profile analysis) to measure the interface width and the lateral correlation length of a surface height function. In particular, we find the correlation length (similar to average terrace size) increases with time during annealing as $t^{1/4}$ at temperatures above 800 K, in agreement with predictions derived for continuous macroscopic surfaces.

PACS numbers: 68.35.Fx, 05.40.+j, 61.14.Hg, 68.35.Ja

Even though the study of the kinetics of flattening of surfaces by annealing was initiated more than 30 years ago in the context of metallurgy [1–4], the same subject is of very much relevance today but in different domains as well. For example, a flat surface is essential for epitaxial growth, and the chemical reactivity of certain catalysts is intimately related to their surface roughness. However, the preparation of a surface having the desired characteristics is still developed largely empirically, so information on the time scales involved in structural reorganization of surfaces is precious.

The kinetics of the flattening of macroscopic surface structures during thermal annealing has been used extensively to determine atomic diffusion coefficients at surfaces [5]. The observed decay time t of a shallow sinusoidal groove has been found to depend on the wavelength λ of the structure as $t \sim \lambda^4$ when surface diffusion dominates mass transport. This result was predicted by Herring [6] and Mullins [2] to result from the curvature-induced surface diffusion current in a conserved, isotropic system. Similarly, the horizontal length scale associated with a bump or hole of general shape is predicted to increase as $t^{1/4}$.

At temperatures below the surface roughening transition, faceting has been observed as a macroscopic profile is annealed [7,8]. This has been interpreted theoretically in terms of the anisotropy of the surface tension near a low-index surface orientation [9]. The $t \sim \lambda^4$ law is still expected in the continuum theory [8], but solid-on-solid (SOS) model simulations suggest $t \sim \lambda^6$ [10]. A related phenomenon—the growth of 3D clusters of average diameter l on a surface by Ostwald ripening—is found to follow the growth law $l \sim t^{1/4}$ when surface diffusion is the kinetically limiting process [11].

Previous work on flattening kinetics had concentrated on the annealing of longer range structures ($\sim \mu\text{m}$), until a recent study of smoothing kinetics of the Cu(100) surface after Cu deposition, for which the growth law for the terrace width $L \sim t^{1/3}$ at early times and $L \sim t^{1/5}$ at later times was found [12].

In this Letter, we report on a similar study of the dynamics of flattening of a TiO₂(110) surface, over atomic length scales up to several hundred angstroms, after the

surface has been roughened by the common preparation procedure of sputter cleaning by argon ion bombardment. Using high resolution low energy electron diffraction (HRLEED) methods, we analyze the diffraction spot profiles to obtain measures (to be defined later) for the width of the solid-vacuum interface and the lateral correlation length. The latter quantity is measured as a function of time to monitor the annealing kinetics. Except at the lowest annealing temperature we used, we find the exponent describing the flattening is near 1/4, in agreement with Mullins's result, but in contrast to the Cu(100) experiment mentioned above.

The (110) TiO₂ (rutile) surface is a well-suited model system for this study. It is studied widely as a catalyst, and its bulk properties are fairly well known [13]. Also, being relatively unreactive to contamination in ultrahigh vacuum (UHV), it is ideally suited for clean surface studies. The (1 × 1) (110) surface is the most stable one, and we observed no reconstruction in vacuum at the temperatures used in this study (up to 950 K), although a (1 × 2) structure has been observed by others [14–16] after certain preparation conditions, in addition to the (1 × 1).

The experiments were performed in an UHV chamber with a base pressure of less than 10^{-10} torr. The TiO₂ sample was a disk of 1 cm diameter and thickness 0.9 mm, sawn and polished [17] to within 0.2° [18] of the (110) orientation. The detailed operation of the type of HRLEED instrument used (Leybold/Specs SPALEED) has been described elsewhere [19]. LEED spot profile measurements in this study were performed at a resolution of at least 0.006 \AA^{-1} in reciprocal lattice space. Heating was done radiatively with a tungsten filament positioned behind the sample and the temperature was controlled with two thermocouples, one glued on the top near the sample edge and the other on the side of the sample. An argon ion sputter gun was used to clean and roughen the crystal surface. Auger electron spectra of the surface were made with a single-pass cylindrical mirror analyzer (CMA) to monitor surface composition. In the region of the surface used for the LEED studies, impurity levels were less than 0.5% of the Ti, O Auger peak intensities, except for a residual concentration of embedded argon which gave Ar(LMM)/O(KLL) peak intensity ratios of between 0.7%

and 2% after annealing, depending on annealing temperature. Additional experimental details may be found in Ref. [20].

After argon ion sputtering, the surface is oxygen deficient but near stoichiometry is restored through the diffusion of the oxygen present in the bulk when annealing above 675 K in vacuum [13], coinciding with the appearance of a (1×1) LEED pattern, although the surface is still quite rough. At an electron energy corresponding to an “out-of-phase” condition, surface terraces separated in height by a single atomic step contribute destructively to the diffraction intensity, resulting in a broad, low spot profile indicating an average terrace width of only a few lattice spacings. On the other hand, diffraction spots at in-phase conditions are already extremely narrow, with full width at half maximum (FWHM) of 0.005 \AA^{-1} due partly to instrument resolution and indicating (1×1) order over an average length scale (defined as $2/\text{FWHM}$ [21]) of at least 400 \AA . Annealing to higher temperatures causes the out-of-phase spots to sharpen, with the in-phase spots unchanged. The flattening process at temperatures above 700 K is therefore dominated solely by the reduction in the density of atomic height steps. Furthermore, by looking at the period in the oscillation of the relative weight of the Bragg peak in the total spot intensity [22–24], scanning energy between in-phase conditions, we conclude that the steps at the surface are predominantly of single height $d = a_{(100)}/\sqrt{2} \cong 3.3 \text{ \AA}$ [20].

Angular profiles of the $(0,0)$ LEED beam after annealing for 20 min at the temperatures 750, 800, and 850 K are shown in Fig. 1, at an electron energy of 151 V corresponding to an out-of-phase condition. Each of the diffraction profiles is clearly composed of (i) a sharp, central Bragg peak $I_{\text{br}}(\vec{k})$ representing only a small fraction of the total integrated scattering intensity, and (ii) a broad “shoulder” profile $I_{\text{sr}}(\vec{k})$.

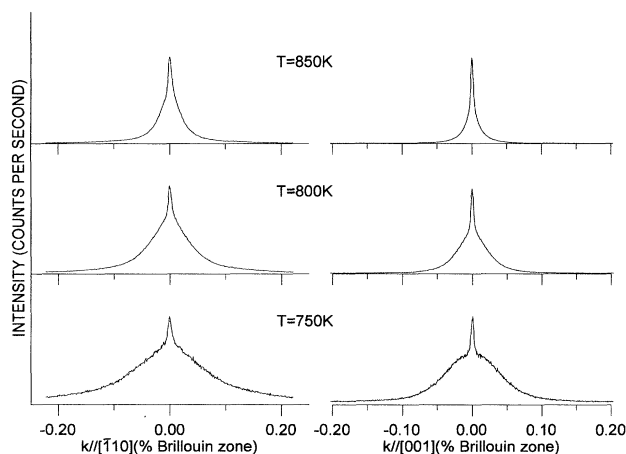


FIG. 1. Angular profiles of the $(0,0)$ beam at the out-of-phase condition $E = 151 \text{ eV}$. The long-range and short-range parts of the intensity are clearly visible. The Brillouin zone width is 0.97 \AA^{-1} .

These two features are understood by examining the structure factor of the surface, which is adequate to describe the relative intensities measured in reasonably narrow LEED spot profiles, since multiple scattering is short ranged. In this (kinematical) approximation, the diffraction intensity as a function of momentum transfer \vec{k} is proportional to [20,24,25] $I(\vec{k}) = I_{\text{br}}(\vec{k}) + I_{\text{sr}}(\vec{k})$, with I_{br} and I_{sr} defined as follows. The Bragg peak intensity $I_{\text{br}}(\vec{k})$ is proportional to the long-range average $\langle \sigma \rangle^2$ of the surface height function $\sigma(k_{\perp}, \vec{R}) \equiv e^{ik_{\perp}h(\vec{R})}$, which is the phase factor for scattering of an electron through perpendicular momentum transfer k_{\perp} from a unit cell on the surface of height h at lateral position \vec{R} . The shorter-range (“shoulder”) profile $I_{\text{sr}}(\vec{k})$ is the 2D Fourier transform of the correlation function $\langle \delta\sigma(\vec{R})\delta\sigma(0) \rangle$ of fluctuations $\delta\sigma = \sigma - \langle \sigma \rangle$ in the height function. To measure a spot profile, the parallel momentum component (\vec{K}) is scanned, with k_{\perp} nearly constant at the fixed energies used here.

At an out-of-phase condition for steps of height d , the height function takes on values $\sigma(\vec{R}) = \pm 1$ for $h(\vec{R})/d$ referring to an even (odd) terrace level. The width of the short-range profile $I_{\text{sr}}(\vec{K})$ defines the inverse correlation length $L^{-1} = \text{FWHM}/2$ for $\delta\sigma$ [21]. Note that L is of the order of the average terrace size on the surface. The sequence of profiles in Fig. 1 shows larger terrace sizes after annealing at higher temperatures. Profiles in $[\bar{1}10]$ and $[001]$ directions have similar, but not identical widths. At the lower annealing temperatures or early times, the broader diffraction profiles exhibit the twofold symmetry of the underlying lattice, suggesting a somewhat asymmetric average terrace shape. The existence of a small Bragg peak I_{br} in these data at the out-of-phase condition is a finite-size effect—the average order parameter $\langle \sigma \rangle$ would average to zero if the system size were much larger than the terrace widths, as discussed in Ref. [20].

The short-range profile shape $I_{\text{sr}}(\vec{k})$ in the $[\bar{1}10]$ direction exhibits approximate scaling behavior over a range of correlation lengths L from 20 to 200 \AA . This was determined by fitting the profiles to the sum of a narrow Gaussian Bragg peak (whose width is partly due to the instrumental resolution) and a broader Lorentzian shoulder $I_{\text{sr}}(\vec{k})$. The Lorentzian form was found to fit this profile over a \vec{K} range out to $\pm 4 \times \text{HWHM}$ in the $[\bar{1}10]$ direction and to $\pm 3 \times \text{HWHM}$ in the $[001]$ direction. A Lorentzian spot profile implies an exponential decay of the (averaged) correlations in $\delta\sigma$ with distance. This form arises, for example, in a random step model on a 1D surface [26], suggesting that step-step interactions play a minor role in the annealing kinetics here.

Time-resolved spot profile measurements were made to determine the evolution of the correlation length L during annealing, and to look for power law growth. Prior to all the kinetics measurements, the surface (at room temperature) was first sputtered with 500 eV argon ions for 1 h at a flux of $\sim 1 \mu\text{A}/\text{cm}^2$, and then preannealed at 700 K for 10 min to allow the argon to desorb and

to restore surface stoichiometry, with flattening occurring over lengths of the order of a few lattice spacings. From this rough initial condition, the sample was then heated at a rate of 5–10 K/s to the annealing temperature which was then maintained constant. Spot profiles of the (0,0) beam at the out-of-phase condition $E = 151$ eV were then collected in the two crystallographic directions at time intervals of 15–60 s, for a period of up to 3 h, as controlled by computer.

Analyzing the profiles in the $[\bar{1}10]$ direction with the fit procedure described above showed a Bragg peak $I_{lr}(\vec{k})$ of constant width and a Lorentzian-like short-range profile $I_{sr}(\vec{k})$ with width $\propto L^{-1}$ decreasing with time and peak height χ growing with time. If there is a scaling law, we should find $L \sim t^\beta$ and $\chi \sim t^\alpha$ with $\alpha = 2\beta$ in 2D, for sufficiently large time t . We define $t = 0$ as the time at which the annealing temperature is reached, at the end of the temperature ramp.

The profile width is shown in Fig. 2 as a function of time. At the upper three annealing temperatures, we find power law behavior with $\beta = 0.23$ – 0.25 . In contrast, annealing at 750 K follows an exponent of $\beta = 0.18 \pm 0.02$ for times $t > 10$ min, with even slower kinetics at earlier times (for which the data are noisier due to low signal levels and faster scans).

The scaling law described above should be altered in cases where the initial correlation length $L(t = 0)$ is not much less than the values of $L(t)$ graphed, to give $L(t)^{1/\beta} - L(0)^{1/\beta} \sim t$ [11,12]. The effects of the initial length $L(0)$ on the exponent analysis are very minor, showing up in early time parts of the 750 and 800 K data, as shown elsewhere [20]. This leads to a very slight increase in the estimate of the exponent β , by 3% at 750 K, 2% at 800 K, and with negligible effect on the higher temperature curves for which $L(t)$ is largest. Secondly, the slight leveling off of the slopes of the 850 and 875 K data in Fig. 2 at late times greater than 1 h is

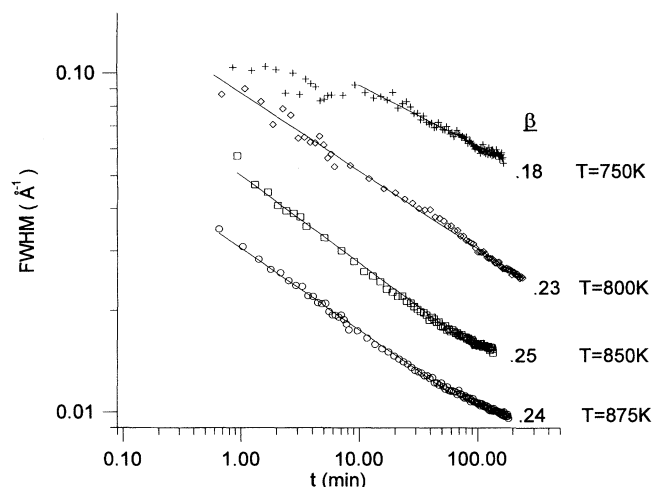


FIG. 2. Width of the short-range profile $I_{sr}(\vec{k})$ vs time t for different flattening temperatures.

not yet fully understood, but may be due in part to finite instrumental resolution. Within these limits, the results above provide a clear demonstration of $t^{1/4}$ flattening kinetics, at temperatures above 800 K.

The peak height data in Fig. 3 directly support the profile width data given above at the temperatures 875 and 750 K; the respective exponents $\alpha = 0.49$ and 0.35 are in excellent agreement with twice the β values found in Fig. 2. On the other hand, the $\chi(t)$ graphs at 800 and 850 K are somewhat curved with slopes varying from about $\alpha = 0.35$ to 0.55 as time increases, in both cases. (Note that the corresponding time dependence of the spot width in Fig. 2 shows only a single exponent β near $1/4$ at both these temperatures.) While the most minor variations seen in the shape of the curves in Fig. 3 are within the limits of accuracy of the spot width measurements, it is clear that the exponent β shifts to lower values at lower temperatures, suggestive of a crossover between shorter- and longer-range scaling regimes.

The origin of the lower value of effective exponent $\beta = 0.18$ found at $T = 750$ K is not yet understood. However, at lower temperatures, one can expect larger possible effects of (i) pinning of steps at point defects (such as at the small residual concentration of embedded argon atoms), (ii) anisotropy of the surface free energy density (simulations below the roughening transition find slower late-time growth [10]), (iii) a change in the kinetics at lower annealing temperatures and very narrow terrace widths due to perturbed local structure [27] and surface atom energetics, including a possible Schwoebel-type effect slowing diffusion over steps [28], and (iv) corrections to both the kinematical scattering approximation and scaling behavior at short length scales.

These results for the $\text{TiO}_2(110)$ surface are markedly different from the measurements of Zuo and Wendelken [12] for $\text{Cu}(100)$, even though our data span about the same range of correlation lengths as theirs. They report an exponent $\beta = 1/5$ at longer length scales in contrast

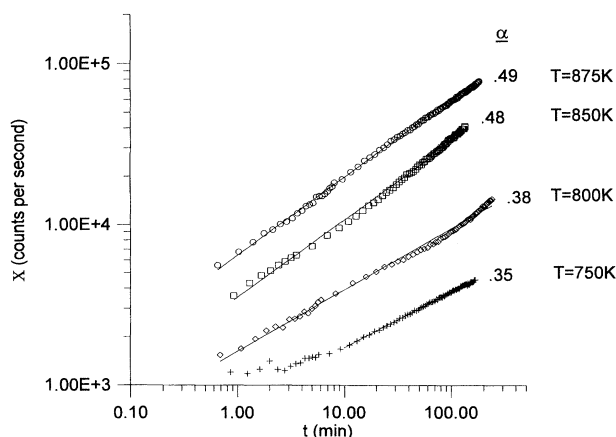


FIG. 3. Peak height $\chi(t)$ vs t for different flattening temperatures.

to the value 1/4 found here, and find β increases to 1/3 at shorter length scales, also in direct contrast to the smaller exponent of 0.18 we find at 750 K. As Zuo and Wendelken point out, an exponent smaller than 1/4 has been predicted from simulations of diffusion-limited kinetics in a bond model [see item (ii) above], or if diffusion is driven by step-step interactions rather than by step curvature [29]. Note that the latter theoretical case, if limited kinetically by atom attachment at steps instead, is predicted to lead to $t^{1/4}$ flattening kinetics, providing an alternate explanation for our results as well. More studies on flattening dynamics will be needed to verify the reasons for the different exponents observed in the TiO₂ and Cu(100) [12] systems.

One may also determine the overall activation energies E for the surface diffusion processes that are responsible for the flattening of the TiO₂(110) surface. For late-time growth following $L \propto (Dt)^\alpha$, with $D \propto e^{-E/kT}$ defining an effective diffusion coefficient, an Arrhenius plot of correlation length versus temperature in the range 750 to 900 K after fixed annealing time gives $E = 2.7$ eV. This value is comparable with activation energies reported for self-diffusion of oxygen in bulk TiO₂ of around 3 eV [30].

In summary, we have observed the dynamics of flattening on the TiO₂(110) surface. We find the exponent describing the time growth of the lateral correlation length, from ≈ 40 to 200 Å and at annealing temperatures ≥ 800 K, to be consistent with the value of 1/4 derived by Mullins [2] for curvature-driven flattening of a continuous system, mediated by surface diffusion, in a long wavelength limit. On the other hand, a smaller exponent describing slower kinetics of annealing at 750 K remains to be explained.

Helpful discussions with G.-C. Wang and G. Vidali are gratefully acknowledged. B. Riel is thanked for his contribution in an early stage of this work. This research was supported by the Networks of Centres of Excellence program and the Natural Sciences and Engineering Research Council of Canada.

-
- [1] C. Herring, in *Structure and Properties of Solid Surfaces*, edited by R. Gomer and C.S. Smith (University of Chicago Press, Chicago, 1952).
 [2] W.W. Mullins, *J. Appl. Phys.* **28**, 333 (1957); **30**, 77 (1959).

- [3] W.W. Mullins and P.G. Shewmon, *Acta Metall.* **7**, 163 (1959).
 [4] J.M. Blakely and H. Mykura, *Acta Metall.* **10**, 565 (1962).
 [5] J.M. Blakely and C.C. Umbach, in *Diffusion at Interfaces, Microscopic Concepts*, edited by M. Grunze, H.J. Kreuzer, and J.J. Weimer (Springer, Berlin, 1988), p. 102.
 [6] C. Herring, *J. Appl. Phys.* **21**, 301 (1950).
 [7] G.E. Rhead, *Acta Metall.* **11**, 1035 (1963).
 [8] K. Yamashita, H.P. Bonzel, and H. Ibach, *Appl. Phys.* **25**, 231 (1981).
 [9] H.P. Bonzel, E. Preuss, and B. Steffen, *Surf. Sci.* **145**, 20 (1984).
 [10] Z. Jiang and C. Ebner, *Phys. Rev. B* **40**, 316 (1989).
 [11] Martin Zinke-Allmang, L.C. Feldman, and M. Grabow, *Surf. Sci. Rep.* **16**, 377 (1992).
 [12] J.-K. Zuo and J.F. Wendelken, *Phys. Rev. Lett.* **70**, 1662 (1993).
 [13] V.E. Henrich, *Rep. Prog. Phys.* **48**, 1481 (1985).
 [14] P.J. Moller and M.-C. Wu, *Surf. Sci.* **224**, 265 (1989).
 [15] G.S. Rohrer, V.E. Henrich, and D.A. Bonnell, *Surf. Sci.* **278**, 146 (1992).
 [16] M. Sander and T. Engel, *Surf. Sci. Lett.* **302**, L263 (1994).
 [17] The crystal was prepared by Single Crystal Technology BV, Enschede, Netherlands.
 [18] Determined by the lack of spot splitting indicative of a vicinal surface, within our LEED instrumental resolution.
 [19] See, for example, U. Scheithauer, G. Meyer, and M. Henzler, *Surf. Sci.* **178**, 441 (1986).
 [20] Bruno Grossmann and Peter Piercy (to be published).
 [21] We define surface correlation lengths as $l = 2/\text{FWHM}$ as is appropriate for an exponentially decaying correlation function $\approx e^{-|x|/l}$. Note that the conventional definition of the transfer width is $T = 2\pi/\text{FWHM}$, as in, e.g., Ref. [22].
 [22] R. Altsinger, H. Busch, M. Horn, and M. Henzler, *Surf. Sci.* **200**, 200 (1988).
 [23] J. Wollschläger and M. Henzler, *Phys. Rev. B* **39**, 6052 (1989).
 [24] H.-N. Yang, G.-C. Wang, and T.-M. Lu, *Diffraction from Rough Surfaces and Dynamic Growth Fronts* (World Scientific, Singapore, 1993).
 [25] J.E. Houston and R.L. Park, *Surf. Sci.* **26**, 269 (1971).
 [26] C.S. Lent and P.I. Cohen, *Surf. Sci.* **139**, 121 (1984).
 [27] H. Onishi and Y. Iwasawa, *Surf. Sci.* **313**, L783 (1994).
 [28] R.L. Schwoebel, *J. Appl. Phys.* **40**, 614 (1969).
 [29] M. Ozdemir and A. Zangwill, *Phys. Rev. B* **42**, 5013 (1990).
 [30] Z.M. Jarzebski, *Oxide Semiconductors* (Pergamon, New York, 1973), p. 224.